PHYSICAL REVIEW D **89,** 075004 (2014)

Gaugino physics of split supersymmetry spectra at the LHC and future proton colliders

Sunghoon Jung[1] and James D. Wells[2]

[1]*School of Physics, Korea Institute for Advanced Study, Seoul 130-722, Korea*
[2]*Physics Department, University of Michigan, Ann Arbor, Michigan 48109, USA*

(Received 20 December 2013; published 2 April 2014)

Discovery of the Higgs boson and lack of discovery of superpartners in the first run at the LHC are both predictions of split supersymmetry with thermal dark matter. We discuss what it would take to find gluinos at hadron supercolliders, including the LHC at 14 TeV center-of-mass energy, and future pp colliders at 100 TeV and 200 TeV. We generalize the discussion by reexpressing the search capacity in terms of the gluino to lightest superpartner mass ratio and apply results to other scenarios, such as gauge mediation and mirage mediation.

DOI: 10.1103/PhysRevD.89.075004 PACS numbers: 12.60.Jv, 14.80.Ly

I. INTRODUCTION

The split SUSY spectrum of lighter fermions and heavier scalars is an attractive possibility [1–4]. Phenomenologically, heavy scalars help to avoid bounds from LHC searches, flavor physics constraints from kaons and B mesons, and limits from electric dipole moments of electrons and neutrons. The 125 GeV Higgs boson mass is accommodated easily by heavy scalars, although some degree of fine-tuning between mass parameters exists in triggering electroweak symmetry breaking (EWSB).

Importantly, split scenarios are not arbitrarily heavy when reasonable assumptions are applied. Too-heavy scalars would induce too-large quantum corrections to the Higgs boson mass. For example, $100(10^5)$ TeV stops can induce 125 GeV Higgs mass for $\tan\beta \sim 5(2)$ [5,6]. Also, too-heavy lightest supersymmetric particles (LSPs) would have too much relic abundance by now. Including Sommerfeld enhancement, a 3.1 (1.0) TeV Wino (Higgsino) LSP can have the right amount of relic density [7,8]. A heavier LSP would be generally constrained—we are ignoring possibilities of conspired mechanisms to dilute relic density. Gauge coupling unification prefers gauginos and Higgsinos to be below 5–50 TeV [3,9].

The general existence of upper bounds on the split spectrum, especially the LSP in the TeV region, may imply that we can test the split scenario as a whole in near-future collider experiments. Scalars of $\mathcal{O}(100\text{–}1000)$ TeV are too heavy for collider discovery, although they may show evidence in future flavor and CP violation measurements in some cases [10]. Indirect detections of heavy Wino dark matter are useful probes [7,8], but they are subject to various uncertainties, including astrophysical ones. We still desire direct probes, and lighter gauginos can play an important role in this endeavor.

Given these conditions, what is really necessary to eventually probe split scenarios up to the relic density upper bounds on LSP masses at a future collider?

Scenarios leading to a split spectrum typically generate gaugino masses from anomaly mediation (AMSB) [11,12]. This is because if, for example, SUSY is spontaneously broken by charged superfields, gaugino masses are prohibited while scalar masses are not. A loop-factor hierarchy between fermions and scalars is generated. Some variants are discussed in Refs. [9,13–15].

We start by discussing the AMSB gaugino model without light Higgsinos. This model is not only generic but provides a simple and clear framework for our analysis whose results become the basis for more general studies. Most simplifying assumptions that we will discuss for collider and cosmological bounds are automatically satisfied in this model. This model may also be the most difficult scenario for the discovery, as the gluino takes on its heaviest value with respect to the Wino mass, and the Winos are degenerate and difficult to find at colliders directly. Thus, studying this scenario can reasonably provide the furthest discovery reach estimation.

After this discussion, we generalize the spectrum and investigate how light Higgsino NLSPs added to the AMSB gaugino spectrum modify the analysis, and how we can apply the results to a general spectrum with variable mass ratios and ordering so that other SUSY breaking mediation models can be studied. Model-dependent cosmological bounds are not considered together. We demonstrate that a useful parameter is the gluino-to-LSP mass ratio, both for the discovery and the discrimination of models.

II. AMSB GAUGINOS WITHOUT HIGGSINOS

A. AMSB spectrum

In the simple model we consider in this section, scalars and Higgsinos are all heavy, and lighter AMSB gaugino masses at leading order (LO) are

$$M_i^A = \frac{b_i \alpha_i}{4\pi} m_{3/2}, \tag{1}$$

where b_i are beta function coefficients. The Wino is the LSP, and the gluino is the heaviest. Next-to-leading order (NLO) results are used in this paper and are plotted in Fig. 1; see the Appendix for how we obtain them. Notably, NLO mass ratios depend somewhat on scalar masses, Higgsino masses, and the overall Wino mass scale which can be important for a split spectrum. With heavy scalars, the Higgsino mass dependence is largest for a small $\tan\beta$—the Higgsino threshold correction, $\delta M_{1,2}(\text{pole}) \sim -\frac{\alpha_{1,2}}{8\pi} 2\mu \sin 2\beta \log\frac{\mu^2}{m_0^2}$, proportional to μ rather than $M_{1,2}$, can be thought of as a renormalization group-induced mixing effect [3]. When $\tan\beta$ is large, heavy squark threshold corrections mainly raise only the gluino mass, thus raising the mass ratio. If scalars are light, effects from Higgsinos and scalars are small—the simplest AMSB models predict scalars as heavy as the gravitino [4,6,12], $m_{3/2}$, but making them lighter is also discussed in light of fine-tuning [11]. Higgsinos heavier than about 50 TeV may be disfavored by gauge coupling unification and are not considered; heavier Higgsinos could have distorted the spectrum more [13,15]. When μ is negative, shown as the blue region in the figures, the Wino gets negative corrections, raising the gluino-to-Wino mass ratio further.

The uncertainty colored bands are spanned by variations of scalar masses ($m_{\tilde{g}} \le m_{\tilde{f}} \le m_{3/2}$) and $\tan\beta$ ($3 \le \tan\beta \le 50$) as well as the renormalization scale ($Q_0/2 \le Q \le 2Q_0$). The central scale is chosen as $Q_0 = M_i^{\text{LO}}(Q_0)$ to minimize a log. The uncertainty from the renormalization scale is smallest among these. The rapid change in the light Wino region is due to gauge coupling running (with Q) mixed with the aforementioned effects.

In this section, we assume heavy $m_{\tilde{f}} = m_{3/2}$ and large $\tan\beta = 50$. Later, we discuss how uncertainties from model parameters can be reflected in the discovery prospect.

Heavy Higgsinos can still help to achieve radiative EWSB. If $m_{H_u}^2$ runs quickly down to an approximate infrared fixed point with the value $-m_{t_{L,R}}^2 < 0$, a similar size of $|\mu|^2 \sim |m_{H_u}^2|$ can trigger EWSB (at least for large $\tan\beta$),

$$m_Z^2 \sim -2(m_{H_u}^2 + |\mu|^2) + 0.5\sin^2(2\beta)(m_{H_d}^2 - m_{H_u}^2), \quad (2)$$

leaving a light Higgs boson

$$\det\begin{pmatrix} |\mu|^2 + m_{H_u}^2 & -B_\mu \\ -B_\mu & |\mu|^2 + m_{H_d}^2 \end{pmatrix} \simeq 0. \quad (3)$$

B. Gluino pair with effective mass

Gauginos are well separated in mass and rarely mix. The LSP is thus nearly a degenerate Wino. Wino production does not generate visible hard objects. Drell-Yan bino production is suppressed, as the bino does not couple to W, Z bosons. In this scenario they are not suitable production modes for discovery at a hadron collider.

Gluino pair production may be the only viable discovery channel at a hadron collider. To begin with, the gluino is assumed to decay as

$$\tilde{g} \to \tilde{w} q \bar{q}, \qquad q = u, d, s, c, b, t \quad (4)$$

via off-shell squarks. It leads to traditional SUSY signatures of jets plus missing energy. We do not distinguish charginos and neutralinos of the same kind because nearly degenerate chargino decays produce only invisibly soft particles.

Decays into top quarks (either into $t\bar{t}\chi_1^0$ or $t\bar{b}\chi_1^-$) are not only possible but can be enhanced if stops are lighter than squarks. However, top quarks are highly boosted in heavy

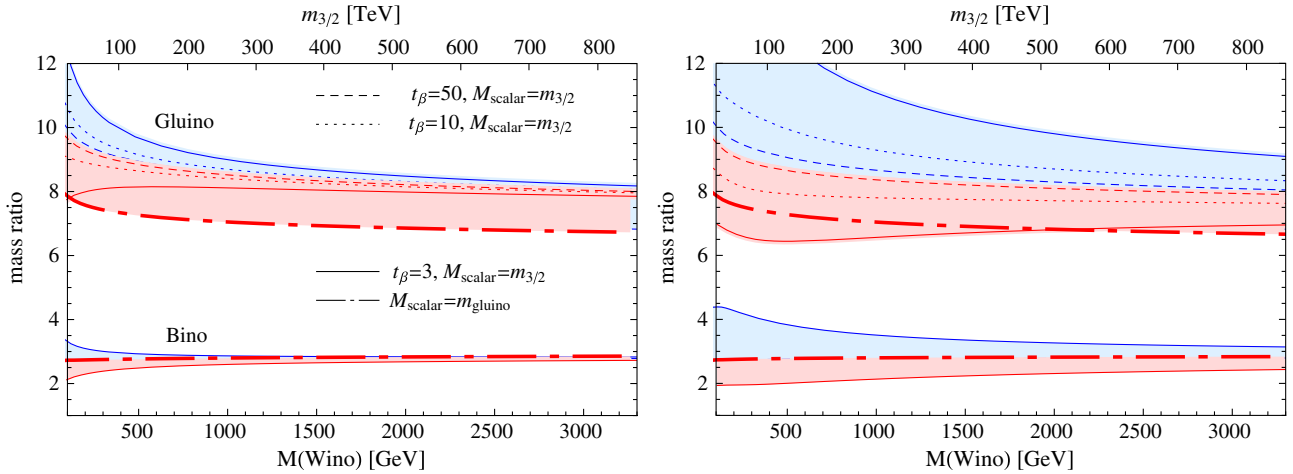

FIG. 1 (color online). AMSB gaugino mass ratios at NLO with Higgsino $|\mu| = 4$ TeV (left panel) and 50 TeV (right panel). Red (blue) lines are with positive (negative) μ. Colored bands are spanned by varying $\tan\beta$ ($3 \le \tan\beta \le 50$), scalar masses ($m_{\tilde{g}} \le m_{\tilde{f}} \le m_{3/2}$) and renormalization scale ($Q_0/2 \le Q \le 2Q_0$). The thick dot-dashed line is with light scalar masses $m_{\tilde{f}} = m_{\tilde{g}}$, and all other lines are with heavy scalar masses $m_{\tilde{f}} = m_{3/2}$. Only a few lines are shown for the bino, for better readability. In the upper horizontal axis, we also show the corresponding $m_{3/2}$ for $\tan\beta = 50$ and $m_{\tilde{f}} = m_{3/2}$.

gluino decays, and top decay products are collimated within an opening angle $\Delta R \sim m_t/p_T(t) \sim 3m_t/M_{\tilde{g}} \ll 0.4$, where 0.4 is our jet radius in the jet algorithm. Thus, without a dedicated top tagging technique applied, the top would look essentially like a single jet. We do not distinguish decays into top quarks from other light quarks in this paper. Likewise, we do not apply b tagging.

Only a small fraction of gluinos decay into intermediate binos. The loop-induced two-body decay, $\tilde{g} \to g\tilde{w}$, is small when the gluino is multi-TeV [16,17]. We ignore these decay modes in this paper.

In all, the assumption of Eq. (4) is reasonable.

It has been widely studied that high-mass supersymmetry can be efficiently probed by variables sensitive to the heaviness and hardness of SUSY particles. One typical example variable is effective mass, $M_{\rm eff}$ [18]:

$$M_{\rm eff} = \sum_i p_T(i) + E_T^{\rm miss}, \tag{5}$$

where the scalar sum runs over all jets with $p_T > 50$ GeV, $\eta < 5.0$ and leptons with $p_T > 15$ GeV, $\eta < 2.5$. Main backgrounds to this analysis are $W + j$, $Z + j$ and a top pair. All signal and background event samples are generated using MadGraph [19] and Pythia [20]. We refer to the Appendix for how to reconstruct physical particles and generate event samples.

The gluino pair production rate is multiplied by a constant K factor 2—no result is available yet, but 2 seems reasonable from Ref. [21]. Background rates are normalized to Pythia-matched cross sections that approximately take into account some of the NLO corrections.

Based on baseline cuts developed by Hinchlifffe and Paige [22], we devise and optimize discovery cuts for 10 TeV gluinos at 100 TeV pp collisions:

(i) At least two jets with $p_T > 0.1M_{\rm eff}$.
(ii) Lepton veto: Definition of an isolated lepton is given in the Appendix.
(iii) $E_T^{\rm miss} > 0.2M_{\rm eff}$ and $p_T(j_1) < 0.35M_{\rm eff}$.
(iv) $\Delta\phi(j_1, E_T^{\rm miss}) < \pi - 0.2$ and $\Delta\phi(j_1, j_2) < 2\pi/3$.
(v) $M_{\rm eff} > cM_{\tilde{g}}$, where a constant c is optimized.

After the first four set of cuts are applied, we optimize the last cut on $M_{\rm eff}$ to maximize statistical significance while requiring at least 10 signal events. See Fig. 2 for the spectrum after the first four cuts. We find the optimal constant $c = 1.5$. We obtain $\sigma_S \simeq 0.072$ fb and $\sigma_B \simeq 0.025$ fb, generating 11 signal events and a statistical significance $\sim$5.5 with 150 fb^{-1}. $S/B \simeq 3$ is well above systematic uncertainties. Dominant backgrounds after all cuts are $Z + j$ and $t\bar{t}$ subdominantly—$W + j$ is suppressed by the lepton veto.

We have also considered more sophisticated variables such as jet mass, $M_J = \sum_{i\in J} m(j_1)$, and (sub)jet counting [23,24]. However, they do not work better than the simple $M_{\rm eff}$ in our case. These variables were designed to work best for a high-multiplicity environment, such as for 10-jet final states. But our gluino pair produces only four quarks at leading order, and these other techniques are not optimal for our low-multiplicity signal.

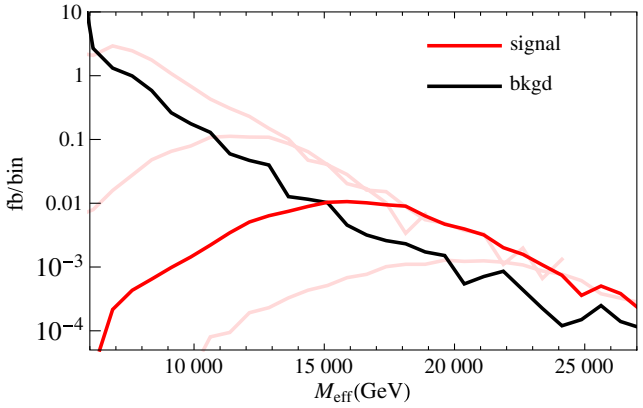

FIG. 2 (color online). Effective mass distribution after our discovery cuts, except for the $M_{\rm eff}$ cut. Several AMSB signals are shown together: dark red from a 10 TeV gluino pair, and light reds from 5, 7.5, 12.5 TeV gluino pairs. Background (black) includes $Z + j$, top pair and $W + j$. The gluino decays as $\tilde{g} \to q\bar{q}\chi_1$. A 100 TeV pp collider is assumed.

C. Scaling rule and discovery reach

Remarkably, the sensitivity to gluino mass scales in a simple way with gluino mass and collision energy. Figure 2 shows that signal-to-background ratios to the right of the signal peak are almost constant after discovery cuts for each gluino mass. This can be understood as gluinos becoming effectively massless at the highest values of $M_{\rm eff}$. Cut efficiencies should also be constant.

If these hold true, a simple scaling rule of the statistical significance can be obtained. The statistical significance of the signal with gluino mass m_i, production rate $\sigma_{\rm Si}$ and luminosity $\mathcal{L}_i$ is

$$\begin{aligned}(\text{significance})_i &= \frac{\sigma_{\rm Si}\epsilon_{\rm Si}}{\sqrt{\sigma_{\rm Bi}\epsilon_{\rm Bi}}}\sqrt{\mathcal{L}_i} \\ &= \sqrt{A_i\epsilon_{\rm Si}}\sqrt{\sigma_{\rm Si}\mathcal{L}_i}\end{aligned} \tag{6}$$

where σ_{B_i} is the total background rate, ϵ_i is the cut efficiency, and $A \equiv \sigma_S\epsilon_S/\sigma_B\epsilon_B$. Since A and ϵ_S stay constant over the interesting range of gluino mass, the statistical significance scales as

$$\frac{(\text{significance})_i}{(\text{significance})_j} = \sqrt{\frac{\sigma_{\rm Si}\mathcal{L}_i}{\sigma_{\rm Sj}\mathcal{L}_j}}. \tag{7}$$

We checked that this scaling rule approximately applies to a wide range of collision energies ($\sqrt{s} = 40$–200 TeV at

TABLE I. Comparison of numerically optimized significance (last column, without parentheses) and the ones obtained from the scaling rule applied to the results in the first row (this estimation is shown in parentheses in the last column).

$\sqrt{s}$	$m_{\tilde{g}}$	σ_S	$\mathcal{L}$	S/B	Statistical significance
100 TeV	5 TeV	21 fb (LO)	5/fb	2.9	12
100 TeV	10 TeV	0.15 fb (LO)	150/fb	3.0	5.5 (5.6)
200 TeV	15 TeV	0.27 fb (LO)	120/fb	3.2	7 (6.7)

least) and gluino masses ($\sqrt{s} = 3$–20 TeV at least) with a split SUSY spectrum; see Table I.

Although it is approximately valid, the scaling rule is very convenient because once sensitivity is estimated for one gluino mass at a certain energy and luminosity, the scaling can be used to predict sensitivities to a wide range of masses, energies and luminosities without needing to repeat lengthy numerical analyses.

Using the scaling rule and gluino pair production rates shown in Fig. 3, we obtain discovery reach contours of the AMSB gaugino model as shown in Fig. 4. The luminosity needed for 5σ statistical significance is contour plotted. The scaling rule is applied to the results optimized for a 10 TeV gluino at 100 TeV LHC, as discussed in the previous subsection. We have ignored systematic uncertainties, which are unlikely to change the results by much; the

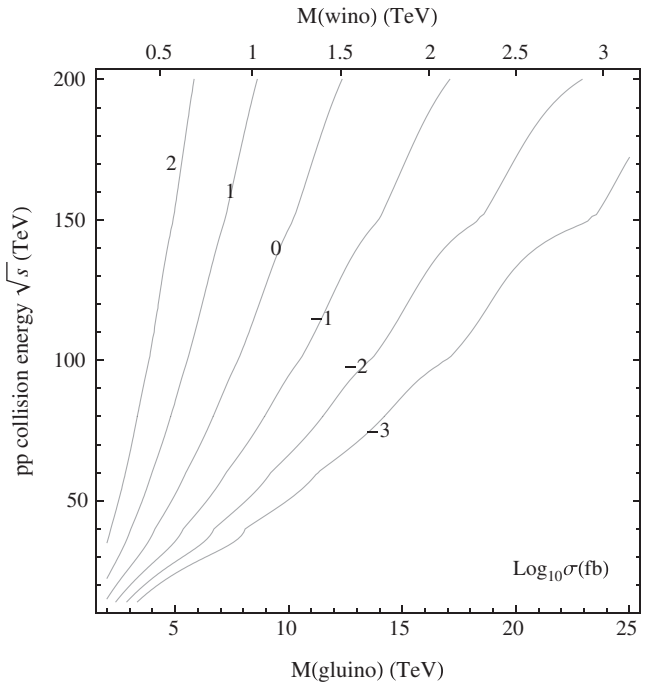

FIG. 3. Gluino pair production rate (fb) at pp collisions. Leading order cross sections. In the upper horizontal axis, the corresponding Wino mass is also shown in the AMSB model with $m_{\tilde{f}} = m_{3/2}$ and $\tan\beta = 50$.

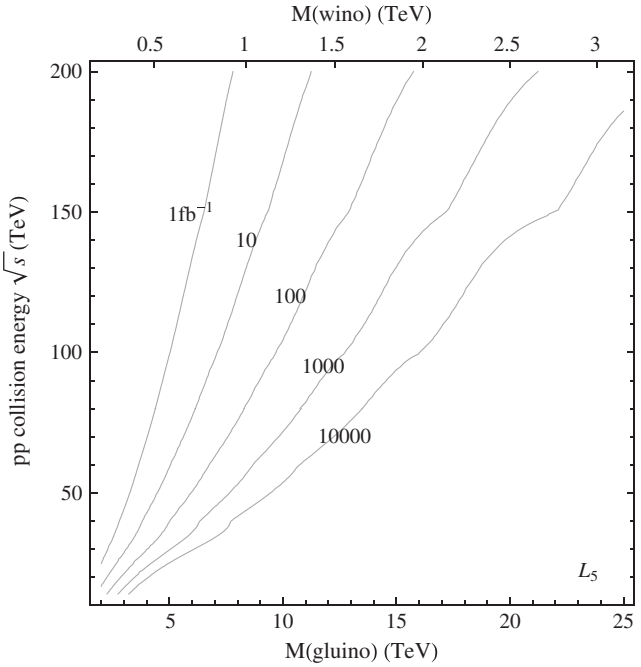

FIG. 4. Luminosity (fb^{-1}) needed to achieve 5σ statistical significance, $\mathcal{L}_5$, is contour plotted. The scaling rule in Eq. (7) is applied. In the upper horizontal axis, the corresponding Wino mass is also shown, as in Fig. 3.

NLO K-factor uncertainty and possible branching ratio suppression can have order-one effects on the production rate (see the Appendix for possible simulation uncertainties). Compared to a recent dedicated study in Refs. [25,26], our significance estimation is a bit more optimistic.

In Fig. 4, we also show the corresponding Wino mass in the AMSB model with $m_{\tilde{f}} = m_{3/2}$. To probe all the way up to a 3.1 TeV Wino LSP, we may need at least a 200 TeV pp collider with $\mathcal{O}(1000)$ fb^{-1} of data. If sfermions are lighter and just as heavy as gluinos, a luminosity of about 2–4 times smaller is needed as the gluino becomes comparatively lighter.

III. GENERAL INTERPRETATION

A. Higgsino NLSP

Our M_{eff} analysis is much more widely applicable, not just to the AMSB model without light Higgsinos. If we allow a light Higgsino NLSP in the AMSB gaugino model, one possible modification is mixing between gauginos and Higgsinos. If $|M_{1,2} - \mu| \gtrsim 450$ GeV with TeV-scale gauginos, the mass splitting between charged and neutral components of Winos/Higgsinos are still kept smaller than 10 GeV, making chargino decays inaccessible. In this limit, multijet final states from gluino productions dominate the most, and this analysis is simplest and most appropriate.

However, a pure Higgsino NLSP can also enable a two-step decay of the gluinos,

$$\tilde{g} \to \tilde{h} jj \to \tilde{w} jjjj \quad \text{where} \quad \tilde{h} \to \tilde{w} + h, W, Z. \tag{8}$$

If Higgsinos are kept far away from Winos, more than 85% of gluino *pairs* will still decay into pure hadronic final states either via one-step (60%–70%) or two-step decays (20%–25%). In the pure hadronic final states, previous $M_{\rm eff}$ analysis can be used with the same set of backgrounds.[1]

Fortunately, two-step decays of the gluino do not modify the $M_{\rm eff}$ spectrum significantly compared to that of one-step decays, as long as the gluino-to-Higgsino mass ratio is greater than about 3. If Higgsinos are closer to gluinos, visible particles are softer while missing transverse energy is smaller, and $M_{\rm eff}$ becomes significantly smaller. The difference, however, resides in how much $M_{\rm eff}$ is contributed from visible particles or missing transverse energy (MET). Two-step decay has more visible particles and smaller MET. This can help to distinguish one-step vs two-step decay using the M_J variable discussed earlier, which is larger for messier two-step decay, but this separate measurement will need much more luminosity.

In all, effects of adding NLSP Higgsinos to the AMSB gaugino model are minimal as long as Higgsinos are far away from gauginos. The small changes in the branching ratios and the $M_{\rm eff}$ spectrum result in a need for about 1.5 times more luminosity for the discovery compared to that shown in Fig. 4.

B. Gluino-to-LSP mass ratio

The $M_{\rm eff}$ spectrum of one-step decaying gluinos is not that sensitive to the LSP mass if the gluino-to-LSP mass ratio is greater than 3. Again, if a LSP is closer to the gluino, $M_{\rm eff}$ becomes smaller and the signal is buried under backgrounds. Thus, the previous results of $M_{\rm eff}$ are valid for any models of gaugino mass (not just to AMSB), as long as these validity conditions and simplifying assumptions are satisfied; otherwise, $M_{\rm eff}$ would not be the right approach for discovery.

This is very useful because we can interpret our results as the discovery reach of the gluino-to-LSP mass ratio in a model-independent way, and the gaugino mass ratio is what is sensitive to the underlying SUSY breaking mediation model. Although different SUSY breaking mediation models may have different golden channels for discovery, we also study others models to illustrate the usefulness of interpreting results in terms of the gluino-to-LSP mass ratio.

Three characteristic patterns of gaugino mass ratios are categorized in Ref. [31] as minimal supergravity (mSUGRA), AMSB and mirage mediation patterns. In this classification, the minimal gauge mediation model (mGMSB) is subsumed under mSUGRA. We consider mGMSB where scalars are relatively light, $m_{\tilde{f}} \sim m_{\tilde{g}}$, and calculate gaugino masses. LO gaugino masses are [32]

$$M_i^G = \frac{\alpha_i}{4\pi} \Lambda_{\rm SUSY}, \tag{9}$$

where $\Lambda_{\rm SUSY} = F/M_m$ in terms of the messenger scale M_m and effective SUSY breaking F term. Here, gauge couplings are grand unified theory (GUT)-normalized so that $\alpha_1 = \frac{5}{3}\alpha_Y$ and $g^2_{\rm GUT} \simeq 0.5$. Gauginos are unified at the unification scale. The mirage mediation pattern is represented as [33]

$$\begin{aligned} M_i^M &= \frac{\alpha_i}{4\pi}\left(\frac{1}{\alpha}\frac{16\pi^2}{g^2_{\rm GUT}\ln(M_{Pl}/m_{3/2})} + b_i\right) m_{3/2} \\ &\simeq \frac{\alpha_i}{4\pi}\left(\frac{1}{0.1\alpha} + b_i\right) m_{3/2} \end{aligned} \tag{10}$$

where $\alpha \sim \mathcal{O}(1)$ is a free parameter and the factor $1/0.1$ arises from KKLT-type models—the notation conforms with that of Ref. [33]. The mirage pattern is effectively an interpolation between the mSUGRA class ($\alpha \to 0$) with $\Lambda_{\rm SUSY} = m_{3/2}/(0.1\alpha)$ and AMSB ($\alpha \to \infty$) patterns, and gauginos are unified at an intermediate value $\alpha \simeq 2$ or at some intermediate energy scale. Thus, mirage mediation models, typically having $\alpha \sim 1$, predict the smallest mass ratios among these models; $0.7 \lesssim \alpha \lesssim 8$ predicts a gluino-to-LSP mass ratio smaller than 3, and our discovery reach will not apply well. But if the mirage pattern is really induced by combination of GMSB and AMSB as in deflected AMSB models [34,35] (instead of KKLT-type models), for example, a wider range of α may be viable.

We use NLO results in this paper and refer to the Appendix for details of our NLO calculations.

Most patterns satisfy our validity conditions and simplifying assumptions—exceptions are mirage mediation with $\alpha \sim 2$, where a compressed spectrum is obtained. In Fig. 5, we interpret the results of Fig. 4 as the luminosity needed for 5σ statistical significance in the gluino-to-LSP mass ratio and LSP mass. We also show AMSB and mGMSB predictions. The mirage pattern, in principle, can predict any value of mass ratio below the AMSB prediction but typically predicts mass ratios smaller than the mGMSB.

The errors of the AMSB are estimated as previously explained. The mGMSB error bands are estimated by varying the renormalization scale and the messenger scale in the range $F/M_m \le M_m \le M_{\rm Pl}$. The lower bound implies that the spurion superfield coupling method of expansion in powers of F/M_m^2 becomes invalid. For the mGMSB, uncertainties from the renormalization scale and the messenger scale are comparable. Again, the main dependence on LSP mass comes from the scale dependence of gauge couplings. Errors of the mGMSB in Fig. 5 are smaller than

[1]Higgsino NLSP production is another efficient discovery mode when light Higgsinos exist [27,28]. But, when Higgsinos are marginally close to Winos, gluinos can be more useful; in addition to $M_{\rm eff}$ analysis (as discussed here), boosted leptons from two-step decays can also be utilized [29,30].

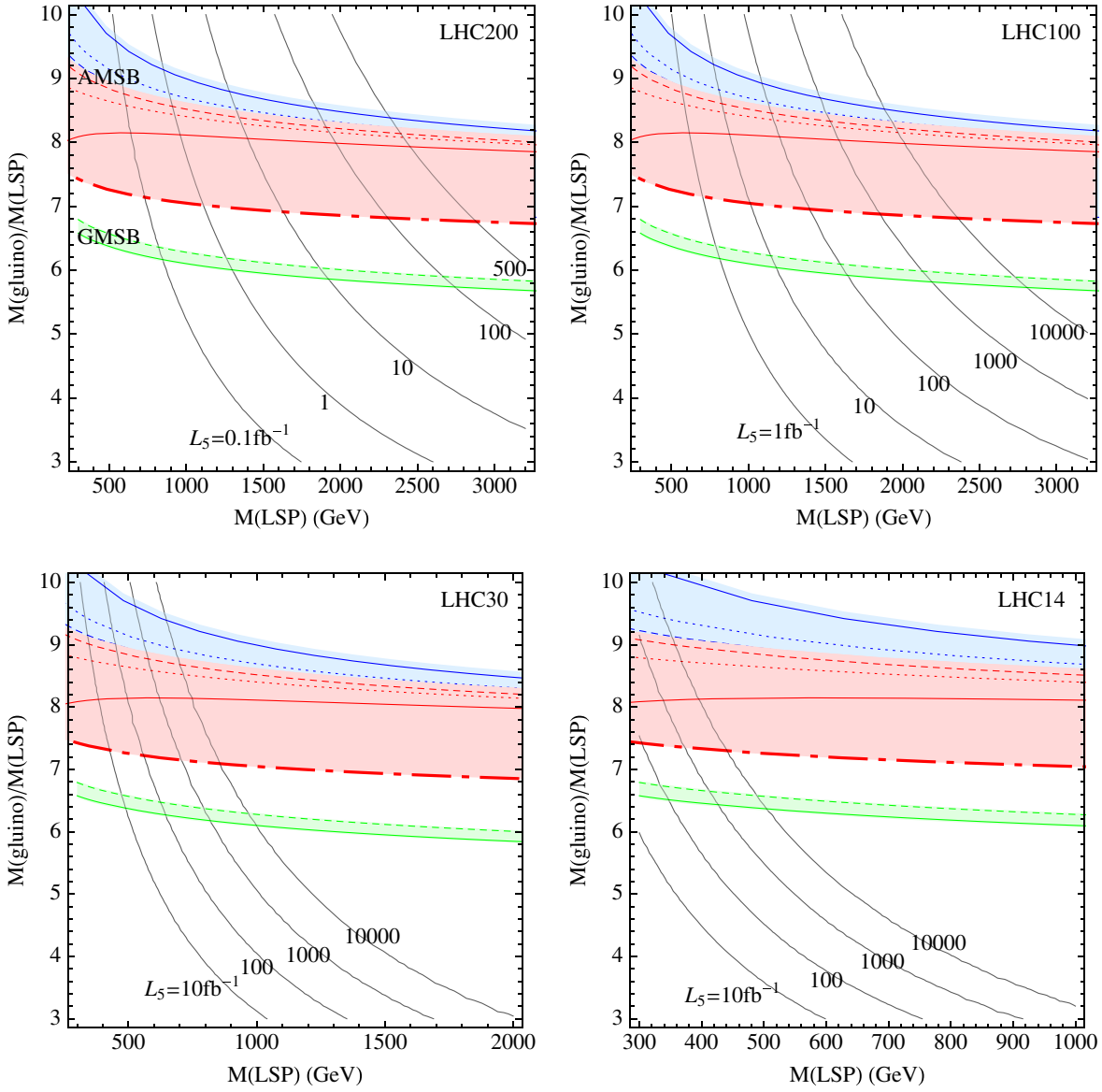

FIG. 5 (color online). Contours of luminosity needed for 5σ statistical discovery, $\mathcal{L}_5$, in the plane of LSP mass and the gluino-to-LSP mass ratio for pp collision energies 200, 100, 30, and 14 TeV. Blue and red regions are AMSB predictions as in Fig. 1 (left panel). mGMSB predictions at NLO are shown in green. Uncertainties of mGMSB are estimated by varying the renormalization scale and the messenger scale [$\Lambda_{\rm SUSY}$(dashed line) $\leq M_m \leq M_{\rm Pl}$(solid line)]. Mirage mediation can, in principle, take any ratio below the AMSB prediction, but $0.7 \lesssim \alpha \lesssim 8$ predicts a gluino-to-LSP mass ratio smaller than 3.

that of the AMSB because scalars are lighter—heavier scalars will modify the mGMSB by a larger amount as well.

Combined with model-dependent cosmological and astrophysical bounds on LSP mass, Fig. 5 can provide a useful discovery prospect of SUSY breaking mediation models. The 3.1 TeV Wino LSP of the AMSB model can be probed at LHC200 with $\mathcal{O}(1000)$ fb^{-1} of data. It should be kept in mind that astrophysical constraints may rule out Winos that make up the full cold dark matter [7,8], including a 3.1 TeV Wino with assumed thermal relic abundance; however, those constraints are dependent on somewhat uncertain halo assumptions and also on absolute stability of the Wino. The Higgsino LSP can also be searched for. If a 1 TeV Higgsino is the LSP in a general spectrum, the 30 TeV LHC can probe up to 6 TeV gluinos (equivalently, mass ratio 6) with $\mathcal{O}(1000)$ fb^{-1}. The 500 GeV bino LSP in the mGMSB, for example, can be probed with 1000 fb^{-1} at LHC14.

The discovery reach in the gluino-to-LSP mass ratio is applicable more generally in a model-independent way. For example, variants of the GMSB where gauginos follow the GMSB relation (with proper NLO corrections) while

scalars feel extra SUSY breaking to become heavier can also be constrained in the same way as the mGMSB. Another example is a scenario with more general nonuniversal gaugino masses at a boundary scale (or the unification scale) that have recently been widely discussed to reduce Higgs mass fine-tuning [36–38]. Although these types of models may not have discussed gaugino mass patterns, this scenario can still be studied with our approach as long as the gluino is much heavier than its decay products.

Another useful property of the $M_{\rm eff}$ spectrum is that the peak location is most sensitive to the gluino mass [18] as long as the gluino is heavier than lighter gauginos and Higgsinos by more than a factor 3; see also Fig. 2. How the gluino decays and the masses of lighter inos are not so important. Thus, the location of a peak can be used to measure the gluino mass. The LSP mass may be measured in precision measurements using leptons in other two-step decays of gluinos as well [18], or by LSP pair production at a future linear collider [39].

IV. CONCLUSION

In conclusion, we have probed the search capabilities of pp hadron colliders for gluinos in the context of split supersymmetry, gauge mediation and mirage mediation. We have found that when the gluino-to-LSP mass ratio is not more than 10—which is expected since gaugino mass ratios are related to each other through their respective gauge couplings or β functions in most scenarios—one can cover the full range of parameters at a 200 TeV collider with approximately 1000 fb^{-1} of integrated luminosity. A 100 TeV collider is not enough energy to fully cover the parameter space. Indeed, perhaps in the most interesting case of Wino LSP thermal dark matter with gauginos satisfying the AMSB mass hierarchy, a 100 TeV collider with even $10,000$ fb^{-1} of integrated luminosity is not enough.

Our analysis has been based on the $M_{\rm eff}$ approach [22], with no special kinematic variables for the signal applied. We did not include third-family tagging analysis, which could be useful if third-family particles are more prevalent in the decays of the gluinos in these scenarios, as might be expected [16,17,40].

On the other hand, there is a vast region of parameter space yet to be explored by the 14 TeV LHC, and by incrementally higher energy colliders, that are still untouched by current experiments and can have dark matter despite not having the standard thermal history [41,42]. Therefore, discovery is possible at any time, but definitive coverage of the Wino LSP scenario through gluino production and decay requires a ~200 TeV collider.

Definitive coverage of the Higgsino LSP scenario is not possible at any collider since supersymmetric gauge coupling unification and thermal dark matter are viable for degenerate Higgsinos at ~1 TeV with all other superpartners arbitrarily heavy. The gluino mass has less reason to be connected *a priori* to the Higgsino mass than it had with the Wino mass. Nevertheless, we consider this to be a somewhat less likely option since the Higgsino mass would alternatively be correlated with the much heavier scalar sector and therefore irrelevant to dark matter concerns and TeV physics, leaving gauginos to play that role. Thus, if it is light, it is likely to be accidentally light and correlated with the gaugino masses, leading to gluino decays to Higgsinos as a viable search option. In this case all of our results apply, and ratios of gluino to Higgsino can be probed much higher than gluino to Wino, only because thermal dark matter Higgsinos are much lighter than thermal dark matter Winos.

Finally, we remark that our analysis is model independent in as much as gluino masses are much heavier than their primary decay products. Given that gaugino masses are often correlated with the gauge coupling strengths and β-function values of their corresponding gauge groups, which are the cases of mSUGRA, mGMSB, AMSB and mirage mediation, this strikes us as a generic prospect.

ACKNOWLEDGMENTS

We acknowledge K. Jung Bae, K. Choi, T. Cohen, S. Hui Im, P. Ko, H. Min Lee, A. Pierce, and Y.-W. Yoon for valuable discussions. S. J. thanks KIAS Center for Advanced Computation for providing computing resources. S. J. is supported in part by National Research Foundation (NRF) of Korea under Grant No. 2013R1A1A2058449.

APPENDIX

1. NLO gaugino masses

LO gaugino masses were presented for the AMSB in Eq. (1), the GMSB in Eq. (9), and the mirage mediation in Eq. (10).

We include NLO corrections to these relations in this paper. Three types of NLO corrections are consistently added. First, NLO corrections to the matching condition at the messenger scale are added for the GMSB. This matching correction does not exist for AMSB, and the relation Eq. (1) is exact to all orders [12]. Including NLO matching corrections, GMSB masses at the messenger scale M_m are given by [43]

$$M_i^G(M_m) = \frac{\alpha_i(M_m)}{4\pi}\left(1 + T_{G_i}\frac{\alpha_i(M_m)}{2\pi}\right)\frac{F}{M_m} \qquad \text{(A1)}$$

where $T_{G_i} = i$ for $SU(i)$ and $T_{G_i} = 0$ for $U(1)$. The gaugino screening theorem is manifest, as the NLO correction is proportional to the gauge coupling itself but not to others.

A second type of NLO correction is to use two-loop renormalization group (RG) equations of the Minimal Supersymmetric Standard Model; we refer to the RG equations in Ref. [44]. Two-loop running resums next-to-leading

logs which are formally the same order as finite one-loop corrections. For AMSB, two-loop parts of b_i in Eq. (1) give dominant corrections to Wino and bino masses [41].

It is these finite one-loop terms that are finally added to complete NLO corrections. This correction defines gaugino pole masses in terms of running gaugino masses. Pole masses are physical observables, and the renormalization scale dependence of gaugino self-energy corrections is canceled by that of gauge couplings (at one-loop level in our case). In this work, we add threshold corrections explicitly by straightforward one-loop Feynman diagram calculations without constructing effective theories. Our calculations are based on Ref. [45] and agree with those of Ref. [46]. We further generalize to the case of different orderings of gauginos and Higgsinos—different orderings have different arguments of threshold log terms.

Mirage gaugino masses are conveniently first matched at the messenger scale of GMSB (or at the Planck scale if mSUGRA), RG-evolved down, and added with threshold corrections to define pole masses.

When sfermions are very heavy, large log terms appear so that a proper low-energy effective theory can be constructed by matching and running, as done in Ref. [3]. However, we are content with observing that this uncertainty, by virtue of not specifying the scalar masses precisely, is not large enough to substantively change our results based on the leading order predictions.

2. Event generation

Generating tails of backgrounds reliably is crucial in this work. For example, at 200 TeV collision, 15 TeV gluino pairs give an effective mass of around 20 TeV, but only $1/10^7$ of $W+j$ backgrounds have this high effective mass.

Similarly to Refs. [23,24,47], we divide phase space with successively smaller cross sections and generate a similar number of events in each sector. We find it useful to use the scalar sum of final state jets to divide phase space in our study. In decreasing order of cross sections, we denote each of the sectors of phase space by P_i. The choice of cross-section ratio $\sigma(P_{i+1})/\sigma(P_i) = 0.9$ seems reasonable and convenient. We generate $W/Z/t\bar{t}+0,1,2j$ backgrounds using MadGraph for each of the following sectors divided in terms of $H_T(j)$ according to the aforementioned cross-section ratio (at $\sqrt{s} = 100$ TeV):

$$W+j\text{: } H_T(j) = \{0,\ldots,700,1500,2800,5200,\ 8800,13800,20500\ \text{GeV}\}, \tag{A2}$$

$$Z+j\text{: } H_T(j) = \{0,\ldots,650,1400,2800,5000,\ 8500,13500\ \text{GeV}\}, \tag{A3}$$

$$t\bar{t}+j\text{: } H_T(j) = \{0,\ldots,750,1500,2600,4300,\ 6700,10000,14500\ \text{GeV}\}. \tag{A4}$$

We omit phase space sectors that are not relevant to multi-TeV ino searches in our study. Other generation-level cuts are jets, $p_T(j) > 50$, $\eta < 5$, and minimal separation between jets and leptons. These cuts improve computation efficiency. On the other hand, signal samples are generated all at once without generation-level cuts.

Up to two additional partons are generated with MadGraph and matched with Pythia parton showered results using a MLM matching scheme [48]. A merging scale **xqcut** $= 50$ GeV is used [49] for all samples. No hadronization nor multiple interactions are simulated. A recent dedicated study including these effects (Ref. [25]) shows a small difference in discovery estimation—ours are somewhat more optimistic though. Our 40 TeV background estimation (generated in the same way) agrees well with the experimental study reported in Ref. [22].

To define jets and isolated leptons in the messy environment of high-energy pp collision, we first jet cluster all energy deposits using FastJet [50] anti-k_T [51] with $R = 0.4$ producing a list of proto-jets. If a proto-jet contains a lepton whose p_T is higher than 50% of the proto-jet's p_T, we assign the proto-jet to be an isolated lepton. All remaining proto-jets are assigned to be normal hadronic jets. There is no detector simulation. Fat jet simulation used to define M_J is carried out with anti-k_T $R = 1.0$.

[1] J. D. Wells, arXiv:hep-ph/0306127.
[2] N. Arkani-Hamed and S. Dimopoulos, J. High Energy Phys. 06 (2005) 073.
[3] G. F. Giudice and A. Romanino, Nucl. Phys. **B699**, 65 (2004); **B706**65(E) (2005).
[4] J. D. Wells, Phys. Rev. D **71**, 015013 (2005).
[5] G. F. Giudice and A. Strumia, Nucl. Phys. **B858**, 63 (2012).
[6] M. Ibe and T. T. Yanagida, Phys. Lett. B **709**, 374 (2012).
[7] T. Cohen, M. Lisanti, A. Pierce, and T. R. Slatyer, J. Cosmol. Astropart. Phys. 10 (2013) 061.
[8] J. Fan and M. Reece, J. High Energy Phys. 10 (2013) 124.
[9] A. Arvanitaki, N. Craig, S. Dimopoulos, and G. Villadoro, J. High Energy Phys. 02 (2013) 126.
[10] W. Altmannshofer, R. Harnik, and J. Zupan, J. High Energy Phys. 11 (2013) 202.
[11] L. Randall and R. Sundrum, Nucl. Phys. **B557**, 79 (1999).

[12] G. F. Giudice, M. A. Luty, H. Murayama, and R. Rattazzi, J. High Energy Phys. 12 (1998) 027.
[13] N. Arkani-Hamed, A. Gupta, D. E. Kaplan, N. Weiner, and T. Zorawski, arXiv:1212.6971.
[14] Y. Kahn, M. McCullough, and J. Thaler, J. High Energy Phys. 11 (2013) 161.
[15] M. Ibe, T. Moroi, and T. T. Yanagida, Phys. Lett. B **644**, 355 (2007).
[16] M. Toharia and J. D. Wells, J. High Energy Phys. 02 (2006) 015.
[17] P. Gambino, G. F. Giudice, and P. Slavich, Nucl. Phys. **B726**, 35 (2005).
[18] I. Hinchliffe, F. E. Paige, M. D. Shapiro, J. Soderqvist, and W. Yao, Phys. Rev. D **55**, 5520 (1997).
[19] J. Alwall, M. Herquet, F. Maltoni, O. Mattelaer, and T. Stelzer, J. High Energy Phys. 06 (2011) 128.
[20] T. Sjostrand, S. Mrenna, and P. Z. Skands, J. High Energy Phys. 05 (2006) 026.
[21] W. Beenakker, R. Hopker, M. Spira, and P. M. Zerwas, Nucl. Phys. **B492**, 51 (1997).
[22] I. Hinchliffe and F. E. Paige, arXiv:hep-ph/0201141.
[23] A. Hook, E. Izaguirre, M. Lisanti, and J. G. Wacker, Phys. Rev. D **85**, 055029 (2012).
[24] S. E. Hedri, A. Hook, M. Jankowiak, and J. G. Wacker, J. High Energy Phys. 08 (2013) 13.
[25] T. Cohen, T. Golling, M. Hance, A. Henrichs, K. Howe, J. Loyal, S. Padhi, and J. G. Wacker, arXiv:1311.6480.
[26] For other studies in the split SUSY context, see for example B. Bhattacherjee, B. Feldstein, M. Ibe, S. Matsumoto, and T. T. Yanagida, Phys. Rev. D **87**, 015028 (2013).
[27] ATLAS Collaboration, arXiv:1307.7292; CMS Collaboration, arXiv:1307.7135.
[28] T. Han, S. Padhi, and S. Su, Phys. Rev. D **88**, 115010 (2013).
[29] G. F. Giudice, T. Han, K. Wang, and L.-T. Wang, Phys. Rev. D **81**, 115011 (2010).
[30] S. Gori, S. Jung, and L.-T. Wang, arXiv:1307.5952.
[31] K. Choi and H. P. Nilles, J. High Energy Phys. 04 (2007) 006.
[32] G. F. Giudice and R. Rattazzi, Phys. Rep. **322**, 419 (1999).
[33] K. Choi, K. S. Jeong, and K.-i. Okumura, J. High Energy Phys. 09 (2005) 039.
[34] A. Pomarol and R. Rattazzi, J. High Energy Phys. 05 (1999) 013.
[35] R. Rattazzi, A. Strumia, and J. D. Wells, Nucl. Phys. **B576**, 3 (2000).
[36] T. T. Yanagida and N. Yokozaki, Phys. Lett. B **722**, 355 (2013).
[37] A. Kaminska, G. G. Ross, and K. Schmidt-Hoberg, J. High Energy Phys. 11 (2013) 209.
[38] S. P. Martin, Phys. Rev. D **89**, 035011 (2014).
[39] H. Baer, T. Barklow, K. Fujii, Y. Gao, A. Hoang, S. Kanemura, J. List, H. E. Logan *et al.*, arXiv:1306.6352.
[40] B. S. Acharya, P. Grajek, G. L. Kane, E. Kuflik, K. Suruliz, and L.-T. Wang, arXiv:0901.3367.
[41] T. Gherghetta, G. F. Giudice, and J. D. Wells, Nucl. Phys. **B559**, 27 (1999).
[42] T. Moroi and L. Randall, Nucl. Phys. **B570**, 455 (2000).
[43] N. Arkani-Hamed, G. F. Giudice, M. A. Luty, and R. Rattazzi, Phys. Rev. D **58**, 115005 (1998).
[44] S. P. Martin and M. T. Vaughn, Phys. Rev. D **50**, 2282 (1994); **78**039903(E) (2008).
[45] D. M. Pierce, J. A. Bagger, K. T. Matchev, and R.-j. Zhang, Nucl. Phys. **B491**, 3 (1997).
[46] A. Gupta, D. E. Kaplan, and T. Zorawski, J. High Energy Phys. 11 (2013) 149.
[47] A. Avetisyan, J. M. Campbell, T. Cohen, N. Dhingra, J. Hirschauer, K. Howe, S. Malik, M. Narain *et al.*, arXiv:1308.1636.
[48] M. L. Mangano, M. Moretti, F. Piccinini, and M. Treccani, J. High Energy Phys. 01 (2007) 013.
[49] J. Alwall, S. Hoche, F. Krauss, N. Lavesson, L. Lonnblad, F. Maltoni, M. L. Mangano, M. Moretti *et al.*, Eur. Phys. J. C **53**, 473 (2008).
[50] M. Cacciari, G. P. Salam, and G. Soyez, Eur. Phys. J. C **72**, 1896 (2012).
[51] M. Cacciari, G. P. Salam, and G. Soyez, J. High Energy Phys. 04 (2008) 063.